Data evaluation technique for electron-tunneling spectroscopy

Vladimir A. Ukraintsev
Department of Chemistry, Surface Science Center, University of Pittsburgh, Pittsburgh, Pennsylvania 15260
(Received 24 July 1995)

A systematic study of local-density-of-states (LDOS) deconvolution from tip-surface tunneling spectra is reported. The one-dimensional WKB approximation is used to simulate the process. A technique for DOS deconvolution from the electron-tunneling spectroscopy data is proposed. The differential conductivity normalized to its fit to the tunneling probability function is used as a method of recovering sample DOS. This explicit procedure does not use unconstrained parameters and reveals a better DOS deconvolution in comparison with other techniques. The advantage of this method is its feasibility for extracting two important physical parameters from experimental tunneling spectra: (i) local surface potential, and (ii) tip-sample distance. These values are the parameters used in the proposed fitting procedure. The local surface potential and the tip-sample distance retrieval are demonstrated by means of numerical simulations. Comparative scanning tunneling spectroscopy is proposed as an approach to eliminate the influence of the tip condition on the surface LDOS recovery.

I. INTRODUCTION

The first observation of the spectral density of electronic states in metal-oxide-superconductor tunneling experiments was made by Giaver.[1] This work led to a reexamination of the one-electron theory of tunneling that has dominated the field for more than 30 years.[2] The new many-body transfer-Hamiltonian approach in tunneling current calculation was pioneered by Bardeen[3] and developed by Cohen, Falicov, and Phillips,[4] Duke, Silverstein, and Bennett,[5] Appelbaum and Brinkman,[6] Caroli *et al.*,[7] and many others.[8] This formalism is used today, in most applications of the tunneling theory.

The invention of scanning tunneling microscopy (STM) by Binnig, Rohrer, Gerber, and Weibel[9] stimulated additional interest in the theory of tunneling. Using the transfer-Hamiltonian formalism,[3] three-dimensional tunneling in the STM was studied by Tersoff and Hamann,[10] Garcia, Ocal, and Flores,[11] Feuchtwang, Cutler, and Miskovsky,[12] and Lang.[13]

With the advent of STM, a scanning tunneling spectroscopy (STS) with atomic spatial resolution became possible. The theory of STS was considered by Feuchwang, Cutler, and Miskovsky,[12] Selloni *et al.*,[14] and Lang.[15] It was concluded that, in the general case of three-dimensional tunneling, current *cannot be calculated* as a simple convolution of sample densities of states (DOS) and tip DOS with the ''effective matrix element for tunneling.'' The simple relation between sample DOS and tunneling current can be obtained in the *one-dimensional* and semiclassical Wentzel, Kramers, and Brillouin (WKB) approximation only.

Selloni *et al.*[14] *qualitatively* generalized the model of Tersoff and Hamann[10] for modest tip-sample voltages and, despite the problem emphasized by Feuchtwang, Cutler, and Miskovsky,[12] suggested convolution of sample DOS and tunneling transmission probability for a crude estimation of the tunneling current. This assumption was justified later by Lang[15] in the specific case of tunneling between Na and Ca single atoms placed on infinite planar metal electrodes. It was shown, by numerical simulation, that the approximation employed by Selloni *et al.*[4] is in reasonable agreement with the ''exact'' solution obtained by three-dimensional many-body transfer-Hamiltonian calculations. To the best of the author's knowledge, this is the only case when the method of tunneling current calculation widely employed today in STM and STS with spatial resolution was confirmed by accurate theoretical calculation.

The first experimental observation of the spectral density of sample electronic states by STM is due to Selloni *et al.*[14] The first derivative of tunneling current over tip-sample voltage or differential conductivity, dI/dV, was used as a measure of the DOS for graphite. Two issues were left unsolved. These are the influence of tip DOS and the effect of the tunneling transmission probability on the observed dependence of the tunneling current on tip-sample voltage.

Stroscio, Feenstra, and Fein[16] proposed an effective solution for the later problem. It was found that, by normalization of the differential conductivity by the total conductivity, one can effectively remove the dependence of the tunneling current on the tip-sample distance. The result was *qualitatively* generalized and it was concluded that this normalization procedure will cancel out both tip-sample distance and tip-sample voltage dependencies of the tunneling transmission probability in the differential conductivity.[17] It was claimed that the $(dI/dV)/(I/V)$ function is ''a relatively direct measure of the surface DOS,''[16] This conclusion was confirmed by Lang[15] in three-dimensional transfer-Hamiltonian numerical calculations for tunneling between Na and Ca single atoms positioned on infinite planar metal electrodes. The normalization technique was also justified by Hamers.[18] Simmon's formulas[19] (WKB approximation) and constant DOS for the tip were used to simulate the tunneling current dependence on the tip-sample voltage. The recovered $(dI/dV)/(I/V)$ function has shown qualitative agreement with the input sample DOS. It is worthwhile to note that in this case[18] less correspondence can be found between input and output sample densities of states in comparison with the ''exact'' simulation done by Lang.[15] It is also important that

in both calculations[15,18] metal-like sample DOS were used.

Stroscio, Feenstra, and Fein[16] experimentally tested the influence of the tungsten tip DOS on the deconvoluted sample density of states. The DOS of a Ni sample, deconvoluted by the $(dI/dV)/(I/V)$ technique, shows no tip-related features. This result contradicts the recently published field-emission electron spectroscopy data of Binh *et al.*,[20] which showed highly structured DOS for tungsten tips with single atom protrusions. To some degree the observation of Stroscio, Feenstra, and Fein[16] is also inconsistent with numerical calculations due to Lang,[13,15] which showed clearly the influence of the tip DOS on the deconvolution result. However, the method developed by Stroscio, Feenstra, and Fein[16] was tested extensively in many experiments and demonstrated reasonable agreement with other experimental and theoretical data.[17,18,21]

The method of DOS deconvolution was modified for measurements on semiconductor surfaces.[22,23] Both the differential and the total conductivities vanish inside the band gap. Therefore, the $(dI/dV)/(I/V)$ function cannot be properly determined. Mårtensson and Feenstra[22] proposed an empirical solution of the problem. The total conductance was broadened by one-pole Fourier low-pass filtering with the pole frequency given by Δ^{-1} (see Ref. 22 and Sec. III A for more detail). If the Δ is larger than band gap, the broadened conductivity becomes then nonzero inside the gap. The broadened I/V provides a more meaningful approximation to the tunneling transmission probability, which is nonzero.[22]

Feenstra[23] has proposed several other empirical modifications of the normalization procedure with the ultimate goal of improving the correspondence between an expected tunneling transmission probability and the modified total conductivity (for details, see, Sec. III A). Finally, Feenstra was able to obtain reproducible and reliable electronic spectra of III-V semiconductors.[23] However, with all these empirical adjustments, it is increasingly difficult to keep explicit the fundamental meaning of the normalization procedure, as well as to justify its ultimate accuracy.

In this paper, a technique for DOS deconvolution from electron-tunneling spectroscopy data is introduced. To recover the sample and/or tip DOS, one may use the *differential conductivity normalized by its fit to the tunneling probability function*. The one-dimensional and semiclassical WKB approximation was used to model electron tunneling between the STM tip and the sample. As shown by simulations, in all studied cases, this technique reveals better deconvolution of the input DOS in comparison with any existing technique.[23] This procedure does not use unconstrained parameters, except the analytical form of the tunneling probability function. Since one should employ the same tunneling model to justify any other DOS deconvolution technique, the suggested procedure is more constrained and certainly more explicit than others.

The advantage of this method is the feasibility of extracting two important physical parameters from experimental tunneling spectra: (i) ''local work function,'' and (ii) tip-sample distance. These parameters are used in the proposed fitting of the differential conductivity by the tunneling probability function. The local surface potential or ''local work function'' and the tip-sample distance retrieval is probed by means of numerical simulation.

Another benefit of the method of DOS deconvolution is the proposed comparative scanning tunneling spectroscopy (CSTS). As shown below, the CSTS virtually eliminates the influence of the tip on the recovered spectra of the surface electronic states.

The fundamental problem of tip-sample spectroscopy is the fact that the tunneling current measured by the STM is a convolution of the sample DOS with the unknown tip density of electronic states. As was shown by Griffith and Kochanski[24] and confirmed in this paper, changes in tip DOS must dominate at negative sample bias (see also Refs. 17, 18, and 25). To diminish the influence of the empty tip DOS on the recovery of the filled sample DOS, the author suggests to analyze the *difference* of the deconvoluted densities of states obtained with the same tip, rather than the individual DOS itself. STM images are very sensitive to the tip condition and, hence, this condition can be precisely monitored.

II. BASICS OF ELECTRON-TUNNELING SPECTROSCOPY

The theory of electron-tunneling spectroscopy has been discussed in many publications.[3–8,12,14,15] Therefore, the goal of this section is to provide a short summary of the theory.

A. Methods of tunneling current calculation

The tunneling current between two weakly bounded electrodes using first-order perturbation theory is[6,10,12]

$$I(S,V)=\frac{2\pi e}{\hbar}\sum_{t,s}|M_{t,s}|^2\delta(E_t-E_s)[f(E_t-eV)-f(E_s)], \tag{1}$$

where V is the sample bias with respect to the tip; S is the tip-surface separation; $M_{t,s}$ is the tunneling matrix element between states ψ_t of the tip and ψ_s of the surface; $f(E)$ is the Fermi-Dirac distribution function; E_t and E_s are the energies of states ψ_t and ψ_s, respectively, in the absence of tunneling. Both energies are referenced to the surface Fermi level. Positive current indicates electron tunneling from tip to surface.

The tunneling matrix element can be calculated as follows, using the method of Bardeen[3]:

$$M_{t,s}=-\frac{\hbar^2}{2m}\int(\psi_t^+\nabla\psi_s-\psi_s\nabla\psi_t^+)d\mathbf{A}, \tag{2}$$

where the integral is calculated over an arbitrary surface lying entirely within the vacuum region separating the tip and the surface.

In the semiclassical WKB approximation, the *density* of the tunneling current between two planar electrodes can be expressed in the following form:[6,10,12]

$$J(S,V)\cong\frac{2\pi e}{\hbar}\left(\frac{\hbar^2}{2m}\right)^2\int_{-\infty}^{\infty}T(S,V,E)[f(E-eV)-f(E)]\rho_s(E)\rho_t(E-eV)dE, \tag{3}$$

where $T(S,V,E)$ is the tunneling transmission probability,[6] $\rho_s(E)$ and $\rho_t(E)$ are the surface and tip densities of electronic states, respectively. In this simplified expression,

the dependence of the tunneling probability on the momentum of the tunneling electron is ignored.

The tunneling transmission probability for a trapezoidal barrier can be estimated in the WKB approximation as[18,21]

$$T(S,V,E)\cong\exp\left\{-2S\left(\frac{2m}{\hbar^2}\left[\overline{\Phi}+\frac{eV}{2}-(E-E_{\parallel})\right]\right)^{1/2}\right\}, \tag{4}$$

where $\overline{\Phi}=(\Phi_t+\Phi_s)/2$ is the average of sample Φ_s and tip Φ_t work functions, $E_{\parallel}=\hbar^2k_{\parallel}^2/2m$ is the component of electron energy parallel to the junction interface, and $k_{\parallel}$ is the corresponding electron momentum.

The tunneling probability is a strong function of the parallel component of the energy $E_{\parallel}$. At each particular total energy E, the DOS with a zero $E_{\parallel}$ component is heavily weighted by the tunneling probability in Eq. (3). Therefore, $\rho_s(E)$ and $\rho_t(E)$ may be approximated by the surface and the tip densities of electronic states with $k_{\parallel}\approx0$.[18] This approximation may in part be a justification for ignoring the tunneling electron momentum in Eq. (3).

One can simplify Eq. (3) at low surface temperature, $k_BT\ll eV$ (k_B is Boltzmann's constant), by using the step function instead of the Fermi-Dirac distribution function. The density of the tunneling current is then

$$J(S,V)\cong\frac{2\pi e}{\hbar}\left(\frac{\hbar^2}{2m}\right)^2\int_0^{eV}T(S,V,E)\rho_s(E)\rho_t(E-eV)dE. \tag{5}$$

Assuming $E_{\parallel}\approx0$ for the electronic states, which influence the tunneling current, the transmission probability can be written in the following form:

$$T(S,V,E)\cong\exp\left\{-2S\left[\frac{2m}{\hbar^2}\left(\overline{\Phi}+\frac{eV}{2}-E\right)\right]^{1/2}\right\}. \tag{6}$$

Expressions similar to (5), (6) were employed in most cases in an attempt to describe semiquantitatively the tunneling spectroscopy with spatial resolution.[12,15,17,18,21] These equations were obtained for the weakly bounded electrodes in the one-dimensional and semiclassical WKB approximation in the limit of the low surface temperature and with a strong preference for tunneling from electronic states with $k_{\parallel}\approx0$. These equations (5), (6) and, hence, these approximations will be used in the following sections to simulate numerically the tunneling current dependency on tip-sample voltage and to test the quality of DOS deconvolution by different techniques.

B. Influence of tip condition on DOS deconvolution

To deconvolute the sample DOS, the first derivative of the tunneling current, with respect to tip-sample voltage (the differential conductivity), is usually analyzed:

$$\frac{dI(S,V)}{dV}\cong A\left[eT(S,V,E)\rho_s(E)\rho_t(E-eV)\Big|_{E=eV}+\int_0^{eV}T(S,V,E)\rho_s(E)\frac{d\rho_t(E-eV)}{dV}dE+\int_0^{eV}\frac{dT(S,V,E)}{dV}\rho_s(E)\rho_t(E-eV)dE\right], \tag{7}$$

where A is a proportionality coefficient related to the effective tip-surface contact area. The second and third terms are usually neglected assuming constant tip DOS and minor changes in tunneling transmission probability at small tip-sample biases.[14,17,18] These simplifications help to explain the basic principle of tunneling spectroscopy, but may lead to qualitatively wrong conclusions. To illustrate this statement, one may express the differential conductivity (7) in the form symmetric with respect to the tip and the surface densities of states. One can accomplish this by substituting $\xi=(E-eV/2)$ in Eqs. (5) and (6). Then the differential conductivity is

$$\frac{dI(S,V)}{dV}\cong\frac{Ae}{2}\left[T'(S,\xi)\rho_s(\xi+eV/2)\rho_t(\xi-eV/2)\Big|_{\xi=eV/2}+T'(S,\xi)\rho_s(\xi+eV/2)\rho_t(\xi-eV/2)\Big|_{\xi=-eV/2}+\int_{eV/2}^{eV/2}T'(S,\xi)\frac{d\rho_s(\xi+eV/2)}{d\xi}\rho_t(\xi-eV/2)d\xi-\int_{-eV/2}^{eV/2}T'(S,\xi)\rho_s(\xi+eV/2)\frac{d\rho_t(\xi-eV/2)}{d\xi}d\xi\right], \tag{8}$$

where

$$T'(S,\xi)\equiv T(S,V,E)=\exp\left[-2S\left(\frac{2m}{\hbar^2}(\overline{\Phi}-\xi)\right)^{1/2}\right] \tag{9}$$

is the appropriate presentation of the tunneling transmission probability (6).

Equation (8) is symmetric with respect to the surface and tip DOS. The $T'(S,eV/2)$ is a probability of tunneling to or from the tip Fermi level and the $T'(S,-eV/2)$ is a probability of tunneling to or from the sample Fermi level. As shown in Fig. 1, at positive V (sample bias with respect to tip) $T'(S,eV/2)\gg T'(S,-eV/2)$. In this case, the differential conductivity can be crudely estimated as

$$\frac{dI(S,V)}{dV}\cong\frac{eA}{2}T'(S,eV/2)[\rho_s(eV)\rho_t(0)+\Delta\rho_s(eV)\rho_t(0)-\rho_s(eV)\Delta\rho_t(0)], \tag{10}$$

where $\Delta\rho_s(eV)$ and $\Delta\rho_t(0)$ are effective changes in surface and tip DOS, respectively, in the proximity of $\xi=eV/2$, where the tunneling probability $T'(S,\xi)$ is close to its maximum value $T'(S,eV/2)$. It will be shown by numerical simu-

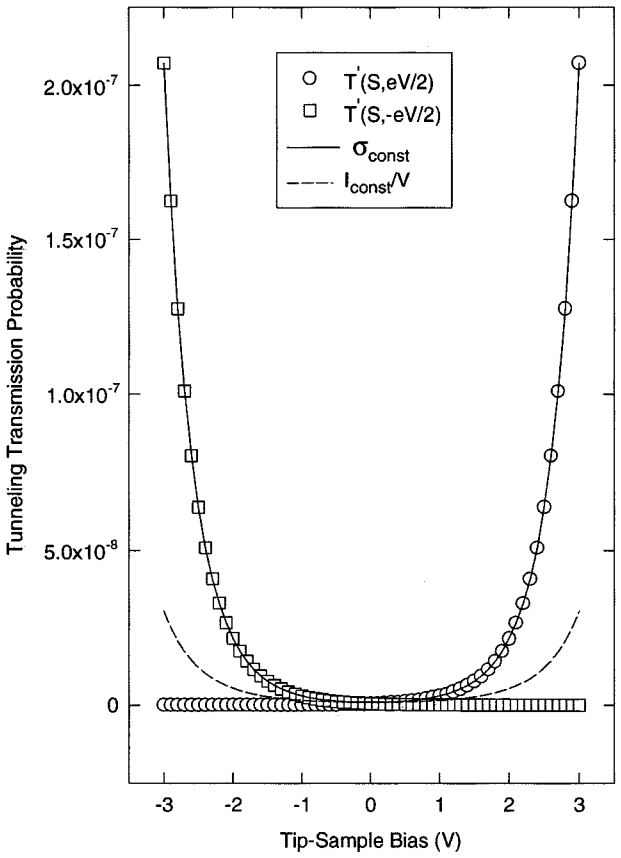

FIG. 1. Dependence of tunneling transmission probability on sample bias with respect to tip. The solid line is the differential conductivity at constant tip and surface DOS (σ_{const}). The dashed line is the $[I_{\text{const}}(s,v)/v]$ function. Circles and squares are the probabilities of tunneling from or to tip and sample Fermi levels, respectively. The equations (9), (12), (13) and values $A=1$, $B=12$ eV$^{-1/2}$, $\Phi=3$ eV, $e=1$ are used in the simulation.

lation that the second and the third terms of Eq. (10) do not vanish. At negative tip-sample voltage, $T'(S,-eV/2) \gg T'(S,eV/2)$, the differential conductivity can be estimated in a similar fashion:

$$\frac{dI(S,V)}{dV} \cong \frac{eA}{2} T'(S,-eV/2)[\rho_s(0)\rho_t(-eV) + \Delta\rho_s(0)\rho_t(-eV) - \rho_s(0)\Delta\rho_t(-eV)]. \quad (11)$$

Equation (11) conclusively demonstrates that the differential conductivity at negative sample biases is proportional to the tip density of nonoccupied electronic states, rather than to the surface DOS. The differential conductivity is proportional to the surface DOS at positive biases only [Eq. (10)]. This problem was discussed qualitatively by Feenstra *et al.*[17,25] and Hamers[18] and the conclusion has been proven by a numerical simulation by Griffith and Kochanski.[24] In Sec. IV, a possible solution of the problem will be considered.

It is worthwhile to mention here the specifics of sample DOS recovery for semiconductors with the Fermi level located in the band gap. In this case, $\rho_s(0) \cong \Delta\rho_s(0) \cong 0$, and the influence of the tip DOS is reduced at negative sample biases (11). Therefore, the sample density of occupied electronic states has a higher chance of revealing itself at negative tip-sample voltages, despite the tunneling probability vanishing [cf. Eqs. (8) and (11)]. This effect will be demonstrated by numerical simulations in Sec. IV.

III. SURFACE AND TIP DOS RECOVERY BY NORMALIZATION TO TUNNELING PROBABILITY

The simplified equations (10), (11) show clearly the method of DOS deconvolution by using the differential conductivity. The best one can do is to normalize the dI/dV to $T(S,eV/2)$ at positive sample bias and to $T'(S,-eV/2)$ at negative sample bias. Then the normalized differential conductivity will be proportional to the sample (10) or to the tip (11) DOS. As also seen from Eqs. (10), (11), one may expect an influence of the first derivatives of the corresponding DOS on the recovered spectra. Nevertheless, all existing methods of DOS recovery from the tunneling spectroscopy data ultimately use this approach.[17,18,21] The difference between various techniques is in the different methods of recovering the tunneling transmission probability.

A. Methods based on total conductivity utilization

As was found empirically in many practical cases,[15,17,18,21] the total tunneling conductivity, I/V, follows reasonably well the desired normalization function. To verify the idea one may analyze the simplest case of constant tip and surface DOS, $\rho_s(\xi)=\rho_t(\xi)=1$. Using (5), (6) and (8), (9) one can obtain algebraic expressions for the total and the differential conductivity, respectively.

The total tunneling conductivity at the constant tip and surface DOS is

$$I_{\text{const}}(S,V)/V = \frac{2A}{VB^2}\left\{ T'(S,eV/2)\left[1+B\left(\overline{\Phi}-\frac{eV}{2}\right)^{1/2}\right] - T'(S,-eV/2)\left[1+B\left(\overline{\Phi}+\frac{eV}{2}\right)^{1/2}\right]\right\}, \quad (12)$$

where $B=2S(2m/\hbar^2)^{1/2}$ is the coefficient proportional to the tip-surface distance S and A is the coefficient related to the tip-surface effective contact area [cf. Eq. (7)].

The differential conductivity at constant tip and surface DOS is

$$\sigma_{\text{const}}(S,V) \equiv \frac{dI_{\text{const}}(S,V)}{dV} = \frac{eA}{2}[T'(S,eV/2)+T'(S,-eV/2)]. \quad (13)$$

The above function (13) appears to be an ideal one for DOS recovery. Indeed, at positive as well as at negative sample biases, it follows closely the appropriate tunneling probability (see Fig. 1). A technique of DOS recovery based on this idea will be discussed in the next section.

As shown in Fig. 1, the total tunneling conductivity at constant tip and surface DOS, $[I_{\text{const}}(S,V)/V]$, does not follow the tunneling transmission probability or the correspond-

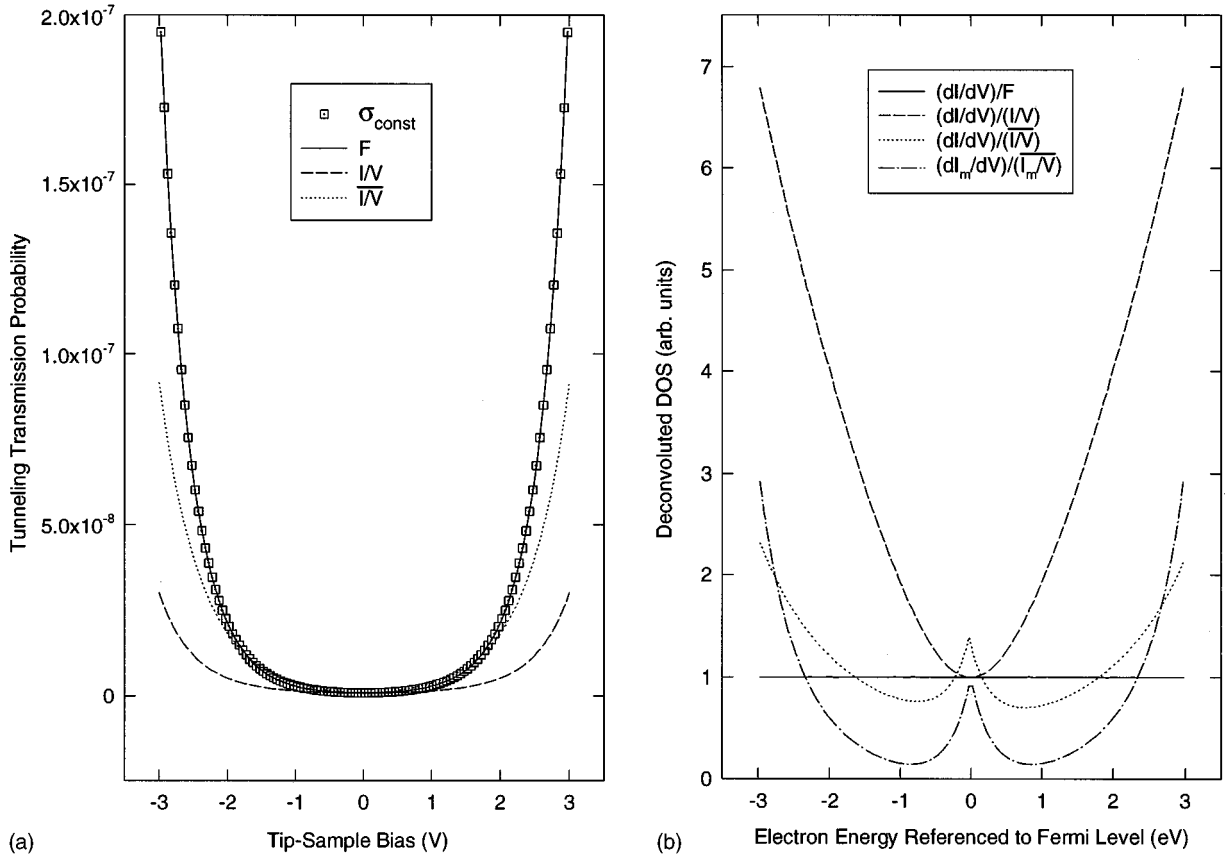

FIG. 2. (a) Approximation of tunneling transmission probability by various functions. The solid line is the fit of the differential conductivity at constant tip and surface DOS (σ_{const}) by the tunneling probability function (F). The dashed line is the total conductivity. The dotted line is the modified total conductivity at the constant tip-sample separation. The equations (5), (6), (13), (14) and values $A=1$, $B=12$ $\text{eV}^{-1/2}$, $\Phi=3$ eV, $e=1$, $\Delta=1$ eV, $a=2.16$ eV^{-1} are used in the simulation. (b) Comparison of different DOS deconvolution techniques. The solid line is the tunneling probability function normalization. The dashed line is the total conductivity normalization. The dotted line is the normalization to the modified total conductivity at a constant tip-sample separation. Dash-dot line is the normalization to the modified total conductivity at variable tip-sample separation (Ref. 23). The equations (5), (6), (14), (16) and values, the same as for (a), are used in the simulation.

ing differential conductivity, $\sigma_{\text{const}}(S,V)$. Hence, normalization of the differential conductivity to the total conductivity will not recover the constant input DOS, $\rho_s(\xi)=\rho_t(\xi)=1$.

Significant deviation from the $\sigma_{\text{const}}(S,V)$ was also obtained for the modified total conductivity [Fig. 2(a)]. In this case, double exponential weighting of the broadened and extended total conductivity was used to approximate the tunneling transmission probability[17,23]

$$\overline{I(S,V)/V}=\exp(a|V|)\int_{-\infty}^{\infty}\frac{I(S,\xi)}{\xi}\exp\left(-\frac{|eV-\xi|}{\Delta}\right)\times\exp(-a|\xi|)d\xi, \tag{14}$$

where a is the best parameter obtained during the $|I(S,V)|$ fitting by the exponential function $\exp(a|V|)$ and Δ is the broadening width. In all simulations $\Delta=1$ eV was used.

Tunneling current versus voltage is always known in a limited voltage range. Hence, to avoid decay of the convoluted total conductivity in the proximity of the limits, one should somehow extend the values of the tunneling current or total conductivity far beyond the limits of the voltage range. For variable tip-sample separation tunneling spectroscopy, Feenstra[23] has suggested extending the current values with constant value equal to the value of current at the largest measured voltage (the extension should be done separately for positive and negative voltages). For constant tip-sample separation spectroscopy, it would be more appropriate to extend the I vs V dependence by its exponential fit. Therefore, this technique was used to extend the tunneling current beyond the voltage limits used in the I vs V simulations at constant tip-sample separation.

With large enough Δ the integral itself [Eq. (14)] is a smooth function of the tip-sample voltage. Therefore, the modified total conductivity (14) is very sensitive to the value of parameter a and, virtually, resembles the fit function $\exp(a|V|)$.

Anyhow, both the procedures used today for the STS data evaluation at constant tip-sample separation show obvious deviations from the tunneling probability function [Fig. 2(a)]. Consequently, normalization of the differential conductivity to these functions should lead to systematic errors during DOS recovery [Fig. 2(b)].

To simulate the DOS recovery in case of STS with variable tip-sample separation, one should use

$$S=S_0+\alpha|V|, \tag{15}$$

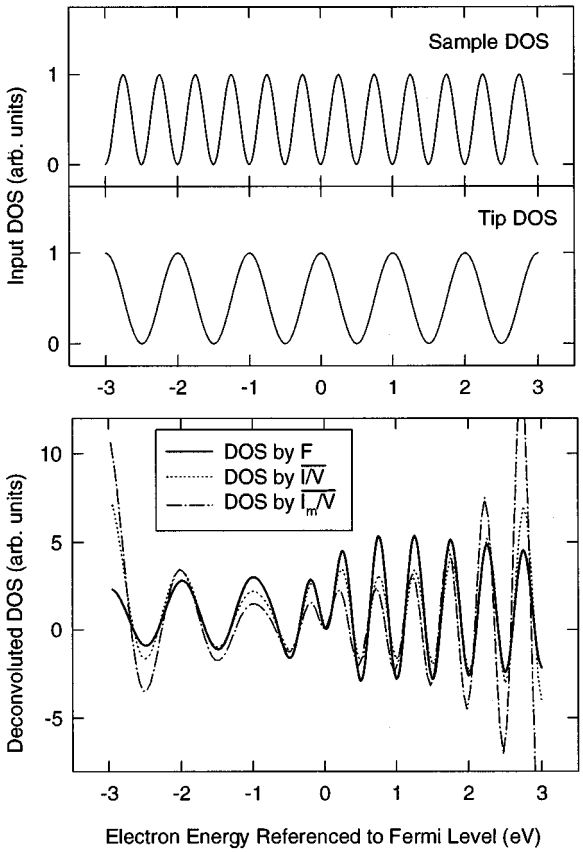

FIG. 3. Tip influence on DOS deconvolution. Top graph: input sample (upper) and tip (lower) DOS. Bottom graph: the solid line is the DOS deconvoluted by F normalization, the dotted line is the DOS deconvoluted by normalization to the modified total conductivity at a constant tip-sample separation $\overline{I/V}$, the dash-dot line is the DOS deconvoluted by normalization to the modified total conductivity at variable tip-sample separation $\overline{I_m/V}$. The equations (5), (6), (14), (16), (17) and values, the same as for Fig. 1, are used in the simulation.

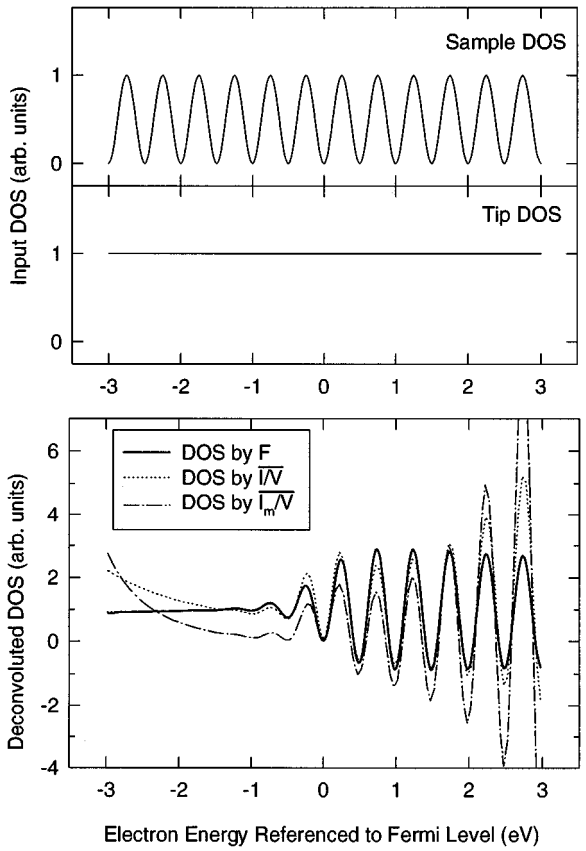

FIG. 4. Problem of sample DOS recovery below the Fermi level. Top graph: input sample (upper) and tip (lower) DOS. Bottom graph: the solid line is the DOS deconvoluted by F normalization, the dotted line is the DOS deconvoluted by normalization to the modified total conductivity at a constant tip-sample separation $\overline{I/V}$, the dash-dot line is the DOS deconvoluted by normalization to the modified total conductivity at variable tip-sample separation $\overline{I_m/V}$. The equations (5), (6), (14), (16), (17) and values, the same as for Fig. 1, are used in the simulation.

where S_0 is the tip-sample separation at $V=0$ V and α is the constant with a typical value of 1 Å/V (Ref. 23). If $\alpha=0.98$ Å/V, then transition from the constant to variable tip-sample separation case can be achieved by a simple substitution:

$$B=B_0+|V|, \tag{16}$$

where B_0 is the coefficient used at constant tip-sample separation.

DOS deconvolution accomplished by normalization of the differential conductivity to the modified total conductivity[23] shows a systematic error in the case of variable tip-sample separation [Fig. 2(b)]. Therefore, in the framework of the one-dimensional WKB simulations, all techniques that employ the total conductivity for DOS recovery reveal significant deviation from the input tip and sample constant densities of states.

B. Method based on differential conductivity fitting

The differential conductivity at a constant tip and surface DOS [Eq. (13)] follows closely the appropriate tunneling probability at positive as well as at negative sample biases (Fig. 1). Therefore, this function is a suitable one for DOS recovery by normalization [Eqs. (10), (11)].

If the sample Fermi level is located inside the band gap, then $\rho_s(0)\ll\rho_t(0)$ and the tunneling differential conductivity should vanish at the negative sample bias [Eq. (11)]. The symmetric tunneling probability function (13) is not appropriate for the fitting of this asymmetric differential conductivity. The situation can be fixed by employing an *asymmetric tunneling probability function*:

$$F(S,V)=A_T T'(S,eV/2)+A_S T'(S,-eV/2), \tag{17}$$

where A_T and A_S are the proportionality coefficients related to the tip-surface effective contact area and proportional to the tip and the sample densities of states at the Fermi level, respectively [cf. Eqs. (10), (11)].

The tunneling probability between the tip and the surface in the semiclassical WKB approximation depends on several parameters: (i) the effective area of tip-surface tunneling contact, (ii) the tip and the sample densities of states at Fermi level, (iii) the tip-surface separation, and (iv) the ''local work function.'' A local surface potential is a more accurate term

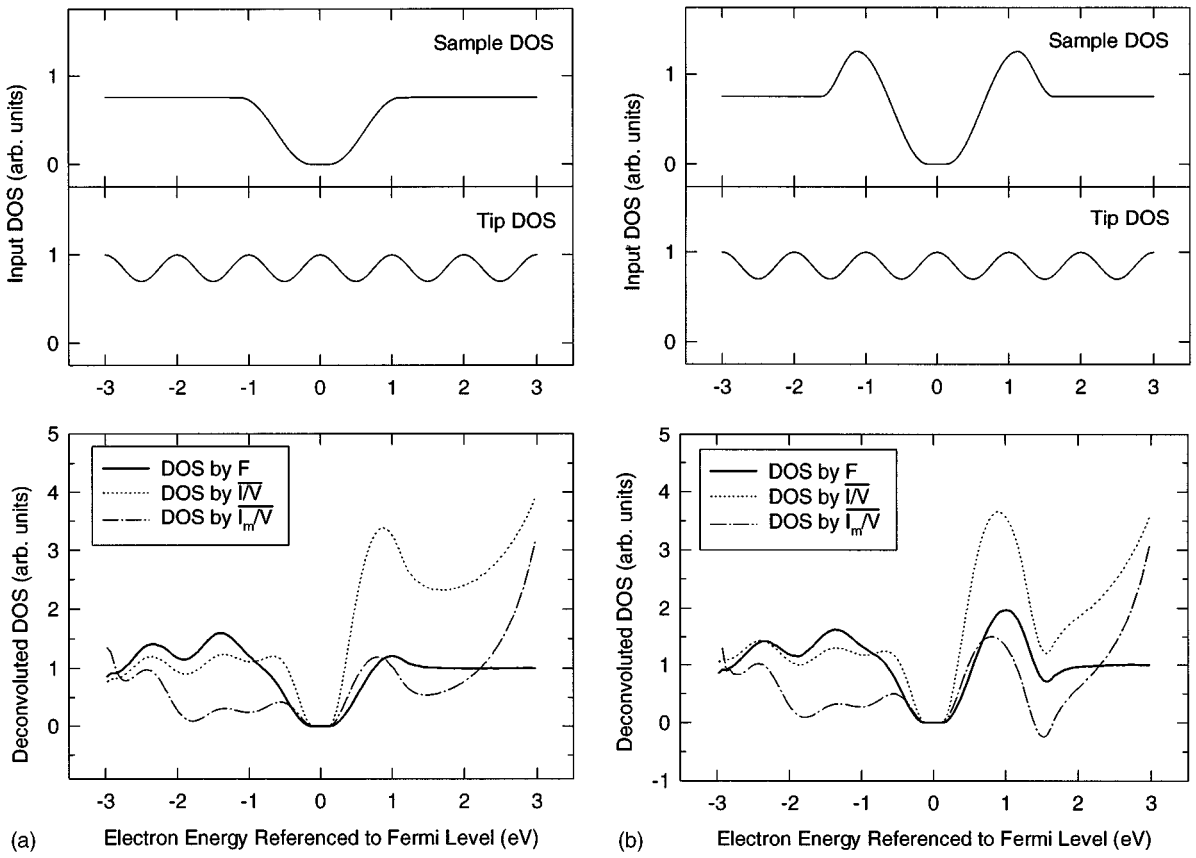

FIG. 5. (a) Deconvolution of the simple semiconductor sample DOS. Top graph: input sample (upper) and tip (lower) DOS. Bottom graph: the solid line is the DOS deconvoluted by F normalization, the dotted line is the DOS deconvoluted by normalization to the modified total conductivity at a constant tip-sample separation $\overline{I/V}$, the dash-dot line is the DOS deconvoluted by normalization to the modified total conductivity at variable tip-sample separation $\overline{I_m/V}$. The equations (5), (6), (14), (16), (17) and values, the same as for Fig. 1, are used in the simulation. (b) Deconvolution of the augmented semiconductor sample DOS. Top graph: input sample (upper) and tip (lower) DOS. Bottom graph: the solid line is the DOS deconvoluted by F normalization, the dotted line is the DOS deconvoluted by normalization to the modified total conductivity at a constant tip-sample separation $\overline{I/V}$, the dash-dot line is the DOS deconvoluted by normalization to the modified total conductivity at variable tip-sample separation $\overline{I_m/V}$. The equations (5), (6), (14), (16), (17) and values, the same as for Fig. 1, are used in the simulation.

for the later value.[26] To extract these parameters from experimental data, one can fit the dI/dV vs V dependence by the analytical functions (17).

The real tunneling transmission probability function may be quite different from this fit, at least because of the three-dimensional nature of tunneling in STM and the strong influence of tip and surface-states dispersion, $E(\mathbf{k})$, on the tunneling probability. The later may cause dependence of the parameters on the energy of electronic states or, in other words, on the tip-sample voltage. The dependence of the coefficient B (tip-surface separation) on the energy of electronic states is also entirely possible. A good example of such dependence might be the spectrum of a buckled dimer on Si(001)-(2×1). As shown by theoretical calculations,[27] the filled ($E_U \sim -0.75$ eV) and empty ($E_D \sim 0.5$ eV) surface states should be strongly localized on ''up'' and ''down'' atoms of the single dimer, respectively. It is predicted that for these ''up'' and ''down'' atoms the difference in normal coordinate is about 0.5 Å. Therefore, for the STM probe placed above the dimer, the density of states of the ''up'' atom of the asymmetric dimer are enhanced in the tunneling spectrum by a factor of 3, with respect to the density of states of the ''down'' one. In this analysis, the decay factor has been assumed to be $k \approx 1$ Å^{-1}.[28]

Therefore, the fitting of experimental differential conductivity $\sigma(S,V)$ by $\sigma_{\text{const}}(S,V)$ and the following DOS recovery cannot be considered to be a quantitative procedure, but rather should be viewed as a *qualitative* one. However, the proposed technique reveals the best DOS recovery, at least in the frame of the WKB simulations.

IV. NUMERICAL SIMULATION OF THE ELECTRON-TUNNELING SPECTROSCOPY, WKB APPROXIMATION, ONE-DIMENSIONAL CASE

In the simulations presented in Figs. 1–6, the following values were used: $B=12$ eV$^{-1/2}$ corresponding to the tip-surface separation of ≅11.7 Å, and the average tip-sample work function $\Phi=3$ eV. Such values were obtained from the evaluation of tunneling spectra of Si(001)-(2×1),[29] and are used here to better model the experimental situation.

In Fig. 3 simulation for a sine tip and a sine surface DOS

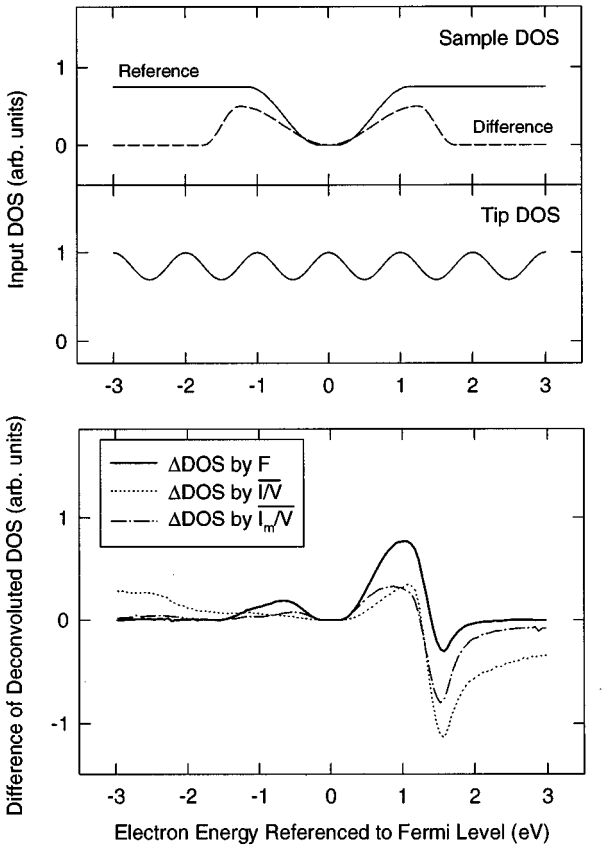

FIG. 6. An example of comparative scanning tunneling spectroscopy. Top graph: input DOS of reference sample (upper solid line), difference between input DOS of probe and reference sample (upper dashed line), and input tip DOS (lower solid line). Input DOS of probe sample is not shown. Bottom graph: the solid line is the difference between probe and reference DOS deconvoluted by F normalization, the dotted line is the difference deconvoluted by normalization to the modified total conductivity at a constant tip-sample separation $\overline{I/V}$, the dash-dot line is the difference deconvoluted by normalization to the modified total conductivity at variable tip-sample separation $\overline{I_m/V}$. The equations (5), (6), (14), (16), (17) and values, the same as for Fig. 1, are used in the simulation.

is presented. The periods of the tip and the sample DOS are 1 and 0.5 eV, respectively. As was expected from Eqs. (10), (11), the deconvoluted DOS resembles the tip DOS at negative sample bias and the sample DOS at positive sample bias. Normalization to the tunneling probability function (solid line) reveals better correspondence to the input densities of states in comparison with normalization to the modified total conductivity at constant (dotted line) and variable (dash-dot line) tip-sample separation. Even if the tip DOS is constant, recovery by any known method would not correctly present the density of sample occupied states (Fig. 4). One can see the systematic error in the sample DOS recovery at negative sample biases.

The situation may be better in the case of a semiconductor sample DOS. As was mentioned in Sec. II B, the influence of tip DOS is reduced at negative sample biases since, for the semiconductor surface, $\rho_s(0)\cong\Delta\rho_s(0)\cong 0$ [Eq. (11)]. The improvement of sample DOS recovery is demonstrated in Fig. 5.

Another considerable difficulty of DOS recovery is seen clearly in Fig. 5. This is the influence of DOS first derivative on the shape of the deconvoluted DOS. This figure demonstrates that the first DOS derivative may cause the appearance of extra features in the spectrum of electronic states. Figs. 3, 4, and 5 illustrate again the better quality of DOS recovery by the proposed technique.

Nevertheless, even in the case of a semiconductor surface, where $\rho_s(0)\cong\Delta\rho_s(0)\cong 0$, the influence of tip DOS on the final result is significant. To diminish the influence of tip DOS, a technique termed *comparative scanning tunneling spectroscopy (CSTS)* is proposed. The effectiveness of tip DOS elimination is demonstrated in Fig. 6. One can see no oscillations at negative sample biases (cf. Fig. 5).

The deconvoluted DOS shown in Fig. 5(a) was used as a reference spectrum. Two features were added to the input DOS of the *reference* sample [Fig. 5(a)] on both sides of the band gap in order to get a *probe* sample input DOS [Fig. 5(b)]. The difference of input sample densities of states (Fig. 6, dashed line) as well as output comparative spectra are presented in Fig. 6. The same tip DOS was used in both simulations.

In the case of an experiment, one should select reference sites. These may be nondefective sites representing the majority of the surface. To get a comparative tunneling spectrum of the specific defected site (a probe), one should subtract the reference deconvoluted DOS (a reference) from the probe spectrum. Both tunneling spectra (reference and probe) should be obtained with exactly the same tip. STM images are very sensitive to the tip condition and, hence, the later can be precisely monitored.

Employment of the tunneling probability function (17) for the comparative site specific tunneling spectroscopy on Si(001)-(2×1) revealed excellent reproducibility on a day-to-day and a tip-to-tip basis.[29] Application of this comparative approach in the case of dI/dV normalization by the modified total conductivity is questionable, partially because of possible changes in local surface potential, tip-surface distance, and effective tip area from one surface feature to another. Accordingly, less reproducible comparative spectra were observed with the later LDOS deconvolution technique in experiments on Si(001)-(2×1).[29]

As mentioned in Sec. III B, two important physical parameters can be extracted from the experimental I vs V curves: (i) the tip-surface separation, and (ii) the local surface potential. In an attempt to retrieve these parameters, the author fitted the dI/dV vs V dependence by the analytical function (17). In Fig. 7, the results of simulations designed to demonstrate such a retrieval are presented.

Figure 7 shows data obtained for the tip and the sample DOS presented in Fig. 5(a). In Fig. 7(a) input tip-surface distance (TSD) is constant, $S\cong 11.7$ Å, and input work function (WF) varies from 2.5 to 3.5 eV. The extracted tip-surface distance (top graph) is almost constant and decreases slightly with the work function. The output WF increases in agreement with input WF (bottom graph).

In the simulations presented in Fig. 7(b) the input WF is held constant at 3 eV and input tip-surface distance is allowed to vary from 9 to 15 Å. The deconvoluted TSD closely follows the input one (bottom graph). The output WF varies moderately around input value of 3 eV (top graph).

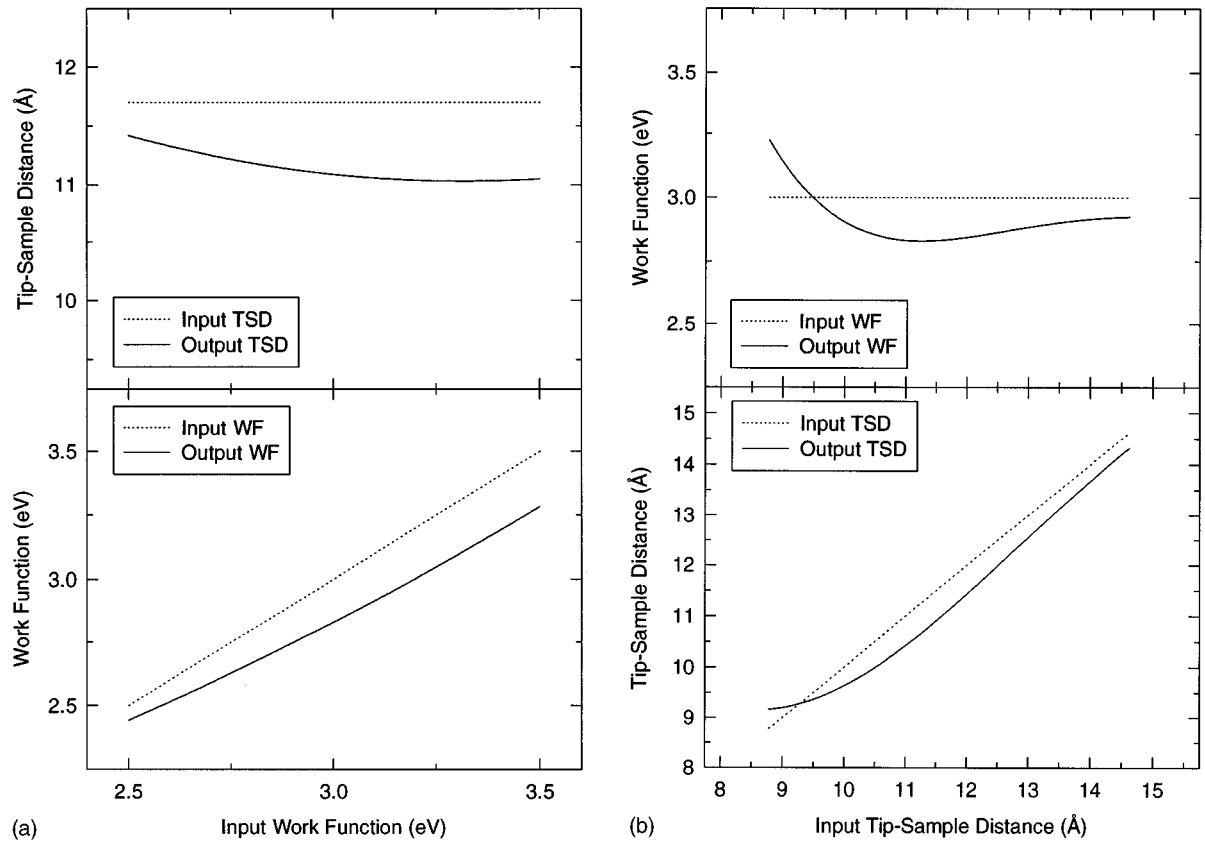

FIG. 7. (a) Work function (WF) and tip-sample distance (TSD) recovery in the case of the simple semiconductor sample DOS. The tunneling current vs tip-sample bias dependencies were fitted by the tunneling probability function (17). Top graph: the solid line is the dependence of recovered tip-sample distance on input work function, the dotted line is the input tip-sample distance. Bottom graph: the solid line is the dependence of the recovered work function on input work function, the dotted line is the input work function. The equations (5), (6), (17) are used in the simulation. (b) WF and TSD recovery in the case of the simple semiconductor sample DOS. The tunneling current vs tip-sample bias dependencies were fitted by the tunneling probability function (17). Top graph: the solid line is the dependence of the recovered work function on input tip-sample distance, the dotted line is the input work function. Bottom graph: the solid line is the dependence of the recovered work function on input work function, the dotted line is the input work function. Equations (5), (6), (17) are used in the simulation.

An accuracy of work function and tip-sample distance retrieval from the simulated I vs V spectra was studied for many other tip and sample densities of states and in most cases discrepancy between the output and the input was below 30% for input WF from 2.5 to 3.5 eV and TSD from 9 to 15 Å. At the same time, slow convergence and larger discrepancy caused by high correlation of the fitting parameters [Eqs. (9), (17)] was observed in some cases of highly modulated tip and sample densities of states. Such situations never occurred during experimental data evaluation.[29]

However, the data presented in Fig. 7 can be considered as a *qualitative example* only. One should clearly realize that all simulations reported here were done in the one-dimensional and semiclassical WKB approximation. The proper test of the method has to be done in experiments or with a much more comprehensive theoretical approach (see Refs. 15, 30).

V. CONCLUSION

A systematic study of surface DOS deconvolution from the tip-sample tunneling electron spectroscopy data was undertaken. The one-dimensional, semiclassical WKB approximation was used to simulate the electron tunneling between the metal tip and the surface. Using the simplest case of constant tip and sample densities of states (Fig. 2), it is shown that all current methods of DOS recovery based on the utilization of the total conductivity have a systematic error. In this paper, a technique for DOS deconvolution from tunneling spectroscopy data is introduced. *The differential conductivity normalized to its fit to the tunneling probability function* is employed as a method of recovering sample DOS. As shown by numerical simulations, this technique reveals a better deconvolution of input DOS, in comparison with the other techniques[23] (Figs. 2–5). The procedure uses no unconstrained parameters, except the analytical form of the tunneling probability function (17).

The advantage of this method is its ability to extract from the experimental tunneling spectra two important parameters: (i) local surface potential, and (ii) tip-sample distance. These values are the parameters used in the proposed fitting procedure. The local surface potential and the tip-sample distance retrieval are probed by means of numerical simulations in the framework of the WKB approximation (Fig. 7). To justify the method, more experimental and theoretical testing

of the technique has to be done. An attempt to apply this method for the analysis of the local density of states of defects on Si(001)-(2×1) has been made.[29]

A method of sample DOS recovery termed *comparative scanning tunneling spectroscopy (CSTS)* is proposed. As shown in Fig. 6, this approach virtually eliminates the influence of tip DOS on the recovered spectra of surface electronic states. The fact that the tunneling current is a convolution of sample DOS, with an unknown tip density of electronic states, causes a fundamental problem for the traditional tip-sample tunneling spectroscopy.

In the case of dI/dV normalization by the modified total conductivity, application of this comparative approach is questionable, partially because of possible changes in the local surface potential from one surface feature to another. The influence of this parameter on the modified total conductivity is unknown.

ACKNOWLEDGMENTS

The author gratefully acknowledges the full support of the Office of Naval Research. I wish to express my deep appreciation to Professor John T. Yates, Jr. for his interest and support of these studies. I also want to thank Dr. R. M. Feenstra and Professor R. J. Hamers for helpful and stimulating discussions.

[1] I. Giaver, Phys. Rev. Lett. **5**, 147 (1960); **5**, 464 (1960).
[2] J. R. Oppenheimer, Phys. Rev. **31**, 66 (1928).
[3] J. Bardeen, Phys. Rev. Lett. **6**, 57 (1961).
[4] M. H. Cohen, L. M. Falicov, and J. C. Phillips, Phys. Rev. Lett. **8**, 316 (1962).
[5] C. B. Duke, S. D. Silverstein, and A. J. Bennett, Phys. Rev. Lett. **19**, 312 (1967).
[6] J. A. Appelbaum and W. F. Brinkman, Phys. Rev. **186**, 464 (1969).
[7] C. Caroli, R. Combescot, P. Noziere, and D. Saint James, J. Phys. C **4**, 916 (1971); **4**, 2599 (1971); **4**, 2611 (1971).
[8] C. B. Duke, in *Solid State Physics Advances in Research and Applications*, edited by F. Seitz, D. Turnbull, and H. Ehrenreich (Academic, New York, 1969), Suppl. 10.
[9] G. Binnig, H. Rohrer, Ch. Gerber, and E. Weibel, Appl. Phys. Lett. **40**, 178 (1982); Phys. Rev. Lett. **49**, 57 (1982); Physica **109/110B**, 2075 (1982); G. Binnig and H. Rohrer, Helv. Phys. Acta **55**, 726 (1982).
[10] J. Tersoff and D. R. Hamann, Phys. Rev. Lett. **50**, 1998 (1983); Phys. Rev. B **31**, 805 (1985).
[11] N. Garcia, C. Ocal, and F. Flores, Phys. Rev. Lett. **50**, 2002 (1983).
[12] T. E. Feuchtwang, P. H. Cutler, and N. M. Miskovsky, Phys. Lett. **99A**, 167 (1983).
[13] N. D. Lang, Phys. Rev. Lett. **55**, 230 (1985); **55**, 2925 (1985); **56**, 1164 (1986).
[14] A. Selloni, P. Carnevali, E. Tosatti, and C. D. Chen, Phys. Rev. B **31**, 2602 (1985).
[15] N. D. Lang, Phys. Rev. B **34**, 5947 (1986).
[16] J. A. Stroscio, R. M. Feenstra, and A. P. Fein, Phys. Rev. Lett. **57**, 2579 (1986).
[17] J. A. Stroscio and R. M. Feenstra, in *Scanning Tunneling Microscopy*, edited by J. A. Stroscio and W. J. Kaiser, Methods of Experimental Physics Vol. 27 (Academic, New York, 1993).
[18] R. J. Hamers, in *Scanning Tunneling Microscopy and Spectroscopy. Theory, Techniques, and Applications*, edited by Dawn A. Bonnell (VCH, New York, 1993).
[19] J. Simmons, J. Appl. Phys. **34**, 1793 (1963).
[20] Vu Thien Binh, S. T. Purcell, N. Garcia, and J. Doglioni, Phys. Rev. Lett. **69**, 2527 (1992).
[21] R. Weisendanger, *Scanning Probe Microscopy. Methods and Applications* (Cambridge University Press, Cambridge, U.K., 1994).
[22] P. Mårtensson and R. M. Feenstra, Phys. Rev. B **39**, 7744 (1989).
[23] R. M. Feenstra, Phys. Rev. B **50**, 4561 (1994).
[24] J. E. Griffith and G. P. Kochanski, CBC Crit. Rev. Solid State Mater. Sci. **16**, 255 (1990).
[25] R. M. Feenstra, Joseph A. Stroscio, and A. P. Fein, Surf. Sci. **181**, 295 (1987).
[26] V. A. Ukraintsev, T. J. Long, T. Gowl, and I. Harrison, J. Chem. Phys. **96**, 9114 (1992).
[27] J. Ihm, M. L. Cohen, and D. J. Chadi, Phys. Rev. B **21**, 4592 (1980); M. A. Bowen, J. D. Dow, and R. E. Alen, *ibid*. **26**, 7083 (1982); M. Schmeits, A. Mazur, and J. Pollmann, *ibid.* **27**, 5012 (1983).
[28] C. Julian Chen, *Introduction to Scanning Tunneling Microscopy* (Oxford University Press, New York, 1993), p. 6.
[29] V. A. Ukraintsev, Z. Dohnalek, and J. T. Yates, Jr. (unpublished).
[30] R. M. Feenstra and J. A. Stroscio, J. Vac. Sci. Technol. B **5**, 923 (1987); J. A. Stroscio and R. M. Feenstra, *ibid*. **6**, 1472 (1988).